Spectrochimica Acta Part A: Molecular and Biomolecular Spectroscopy 286 (2023) 121978

Contents lists available at ScienceDirect

Spectrochimica Acta Part A: Molecular and Biomolecular Spectroscopy

journal homepage: www.journals.elsevier.com/spectrochimica-acta-part-a-molecular-and-biomolecular-spectroscopy

Changes in the mitochondrial membrane potential in endothelial cells can be detected by Raman microscopy

Anna Pieczara [a], Ewelina Matuszyk [a], Piotr Szczesniak [c], Jacek Mlynarski [c], Malgorzata Baranska [a,b,*]

[a] Jagiellonian Centre for Experimental Therapeutics (JCET), Jagiellonian University, 14 Bobrzynskiego Str., 30-348 Krakow, Poland
[b] Faculty of Chemistry, Jagiellonian University, 2 Gronostajowa Str., 30-387 Krakow, Poland
[c] Institute of Organic Chemistry, Polish Academy of Sciences, 44/52 Kasprzaka Str., 01-224 Warsaw, Poland

HIGHLIGHTS

- Visualization of mitochondria and tracking of functional changes in live cells was shown.
- Subcellular mitochondrial activity was tested using labeled and unlabeled Raman imaging, the latter improved sensitivity.
- The MitoBADY Raman probe was used to detect subtle changes in mitochondrial membrane potential as an indicator of mitochondrial activity.
- A semi-quantitative approach was used to estimate mitochondrial activity in live cells.

GRAPHICAL ABSTRACT

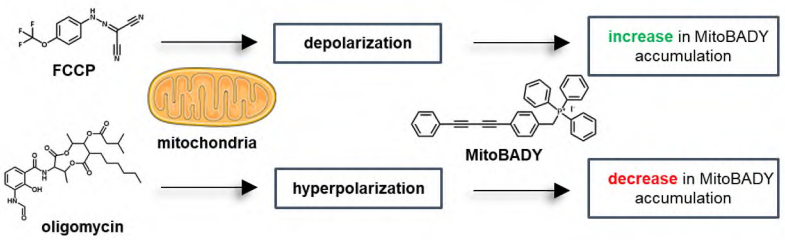

ARTICLE INFO

Keywords:
Mitochondria
Cytochrome *c*
Raman microscopy
Raman probe
MitoBADY
Hormones

ABSTRACT

The role of mitochondria goes beyond their capacity to create molecular fuel and includes e.g. the production of reactive oxygen species and the regulation of cell death. In endothelial cells, mitochondria have a significant impact on cellular function under both healthy and pathological conditions. Endothelial dysfunction contributes to the development of various lifestyle diseases and the key players in their pathogenesis are among others vascular inflammation and oxidative stress. The latter is very closely related to mitochondrial dysfunction; however, it is not straightforward. First, because mitochondria are small cellular structures, and second, it requires a sensitive method to follow the subtle biochemical changes. For this purpose, Raman microscopy (RM) was used here, which is considered a high-resolution method and can be applied *in situ*, usually as a non-labeled technique. In this work, we show that RM can not only locate mitochondria in the cell but also track their functional changes. Moreover, we test if labeling cells with Raman probes (Rp) can improve the specificity and sensitivity of RM (compared to conventional labeled techniques such as fluorescence, and the non-labeled Raman technique). MitoBADY Rp was used to detect changes in mitochondrial membrane potential as an indicator of mitochondrial activity, e.g. hyperpolarization or distortion of the proton gradient in the intermembrane space (depolarization). Thus, we show and compare RM, in the form of a label and non-labeled, to such a subtle cellular analysis.

* Corresponding author at: Faculty of Chemistry, Jagiellonian University, 2 Gronostajowa Str., 30-387 Krakow, Poland.
E-mail address: m.baranska@uj.edu.pl (M. Baranska).

https://doi.org/10.1016/j.saa.2022.121978
Received 3 August 2022; Received in revised form 30 September 2022; Accepted 8 October 2022
Available online 14 October 2022

1. Introduction

All of the arterial vasculature of the heart down to the level of the capillary bed is lined with a monolayer of endothelial cells (EC), thus endothelium is a spatially distributed organ, which plays a significant role in many physiological functions [1]. The endothelium controls e.g., vasomotor tone, blood cell trafficking, hemostatic balance, inflammation, and angiogenesis. Endothelial dysfunction (ED) participates in the development of vascular diseases [2]. Therefore, the ED is a hallmark of atherosclerosis, diabetes mellitus, coronary artery disease, hypertension, and hypercholesterolemia. The special role in the above-mentioned disorders plays the mitochondria-mediated ED. The role of mitochondria goes beyond the production of adenosine-5′-triphosphate (ATP) providing energy, but also is responsible for the regulation of ion homeostasis, generation of reactive oxygen species (ROS), and the activation of programmed cell death [3–5]. Even though mitochondrial content in ECs is modest compared to other cell types e.g. muscle cells [6] mitochondrial dynamics act as a pivotal orchestrator of ECs homeostasis, hence the disturbance of mitochondrial dynamics contributes to ED [7]. Importantly, mitochondria in ECs serve as a sensor of the local environment of the blood including damage signals, e.g. hyperglycemia, aging, or smoking. Subsequently, it leads to oxidative stress, inflammation, and cell senescence leading, e.g. to cardiovascular diseases (CVD).

Although ECs obtain energy mostly from the process of glycolysis [8], still the electron transport chain (ETC) plays a crucial role in the generation of ROS, initiation of apoptosis, and maintenance of Ca^{2+} homeostasis. ETC is a set of protein complexes (I-IV) and electron transporters (ubiquinone and cytochrome *c*), present in highly folded inner mitochondrial membranes. Crucially, ETC activity is one of the factors in ATP production efficiency. Therefore, observing the inequality between ETC activity and the cell ATP requirement may lead to ATP deficiency, inhibition of cell function, and subsequently to overproduction of ROS, development of oxidative stress, and apoptosis dependent on cytochrome *c* release from the mitochondrial membrane. [9,10].

Mitochondria are both targets and mediators of stress [11,12]. Due to stress caused by various factors, the level of hormones in the body changes [13]. It is known that chronic stress is a significant risk factor for CVD, what is more, the endothelium emerges as a primary target for excessive glucocorticoid and catecholamine action [14]. The mechanism underlying the stress-induced ED is still elusive. It is described that mitochondria sense changes in energy demand and rapidly respond to energy-mobilizing glucocorticoids (e.g. cortisol) and catecholamines (adrenaline and noradrenaline) [11]. Cortisol directly decreases nitric oxide (NO) availability and potentially induces the production of proinflammatory cytokines and adhesion molecules. Excessive catecholamines in the bloodstream may induce ROS production and lipid peroxidation as well as increased production of angiotensin II [14].

The most widely used technique for imaging mitochondria is fluorescence microscopy. This technique uses mostly organic fluorophores and immunochemistry. The largest group of fluorescent dyes are small fluorescent particles that accumulate in the mitochondrial space due to the mitochondrial membrane potential (MMP) or interact with molecules that build it, e.g. cardiolipin [15]. Marker-free imaging of mitochondria function in their native microenvironment is possible as a result of the autofluorescence of NADH [16]. However, most staining protocols are designed for live-cell imaging. Imaging of mitochondria in fixed cells is limited to immunochemistry [15]. RM does not require staining, and due to the unique spectral signature of the endogenous heme group of cytochrome *c* obtained in Raman resonance conditions, it allows the detection of these small organelles. It enables real-time measurements and monitoring of physiological parameters for live cells [17].

There are several methods to obtain information about a normal and disturbed mitochondrial function, including an analysis of ATP production, staining of changes in MMP (JC-1, MitoTracker), or measurement of oxygen consumption rate. In turn, Raman microscopy allows for tracking changes in cytochrome *c* redox state that can be considered as a marker of mitochondrial activity. Cytochrome *c* is a soluble hemoprotein present in mitochondria and acts as an electron carrier from complex III to complex IV in ETC. It has been shown that monitoring the state of cytochrome *c* using Raman microscopy is much faster than the standard cell viability test (MTT), while comparing the results for ATP measurements or JC-1 staining, they were very similar [18]. Importantly, resonance Raman spectroscopy (rRS) is sensitive to proteins containing heme groups. Based on the Raman spectrum, the form of cytochrome *c* can be determined, i.e. oxidized *vs* reduced [19]. Like any other technique, RM has its limitations, e.g. in quantitative analysis when the measurement is taken in resonance conditions and, in some cases, limited identification of sample components resulting from overlapping of Raman bands [20]. To overcome these and other limitations, another approach in subcellular studies is the introduction of so-called Raman probes (Rp), which stands as a labeled variant of RM [21]. It has been shown that it improves selectivity and sensitivity in some subcellular analyses. The RM supported by Rp relies on the use of small molecules that gives the characteristic signal in a biologically silent region (i.e. 2800 – 1800 cm^{-1}) of the Raman spectrum [22]. A careful and well-thought-out design of the Rp allows the identification of many cell organelles simultaneously [23,24].

Raman microscopy is becoming an attractive tool in cell biology for visualization and monitoring intracellular processes, which can be an alternative to standard fluorescence. Raman spectra are more informative than fluorescence because they provide information about changes occurring throughout the cell, not just in one organelle. A Raman image shows how certain organic compounds are distributed in a cell, including proteins, lipids, nucleic acids, and cytochrome *c* [25–27]. Furthermore, common fluorescent probes are relatively bulky and often considerably alter biological activity when used to tag small biomolecules. In addition, fluorescent probes are not usually suitable for multiplex detection of more than three targets because of their broad spectrum [28], which is not a problem in Raman imaging utilizing probes to visualize the cellular organelles, i.e. nucleus, mitochondria, and endoplasmic reticulum [29]. Therefore, developing labels with better information content, minor perturbation, high specificity, and sensitivity is a critical subject in current biological research [28].

More and more research is being reported on Rp targeting numerous compounds in the cell, e.g. DNA [30], RNA [31], proteins [31], lipids [32], as well as whole organelles [24,29,33]. It is a very attractive and future-oriented topic, that will allow expanding the knowledge of cell biology. MitoBADY (Fig. 1) was the first Rp shown to accumulate in the mitochondria of HeLa cells [33]. Targeting of mitochondria by MitoBADY is based on the presence in its structure of the lipid-soluble triphenylphosphonium cation (TPP^+), which is transferred electrophoretically to the mitochondria thanks to their polarized membrane [34].

In this paper, we verify the hypothesis that MitoBADY can track changes at the subcellular level associated with mitochondria dysfunction accompanying ED. The aim is, therefore, firstly, to optimize the conditions for using MitoBADY for the detection of mitochondria, and MMP, as an indicator of mitochondrial activity. For this, ECs were

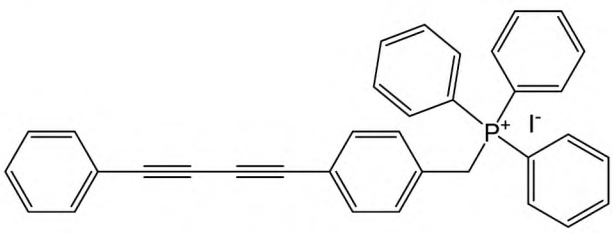

Fig. 1. The structure of MitoBADY.

incubated with MitoBADY and treated with various agents, i.e., FCCP, rotenone, antimycin A, oligomycin, and sodium azide. Moreover, to understand the effects of stress hormones on the ECs, several of them were tested, including adrenaline, noradrenaline, cortisol, and an equimolar mixture of hormones.

2. Materials and methods

2.1. Cells culture

Primary human aortic endothelial cells (HAEC) were cultured in supplemented endothelial growth medium (EGM-2MV from Lonza). The cell culture was incubated at 37 °C, 5% CO_2/95% in the air humidified cell culture incubator. HAEC were seeded directly onto CaF_2 windows, in the amount of approximately 150 000 per slide, after time enough for cells to proliferate and spread, enabling them to reach optimal confluence. Prior Raman imaging cells were treated depending on experiments, with MitoBADY (50 – 400 nM, 15 – 60 min), FCCP (0.7 μM, 5 min), oligomycin (1 μM, 30 min), rotenone (1 μM, 30 min) with antimycin A (1 μM, 30 min), adrenaline (5 μM, 30 min), noradrenaline (5 μM, 30 min), cortisol (5 nM, 30 min), and their equimolar mixture (5 μM for adrenaline, noradrenaline and 5 nM for cortisol, 30 min) (Sigma-Aldrich).

2.2. Raman measurement

Raman imaging was accomplished using WITec Confocal Raman Microscope (WITec alpha 300), operated *via* WITec Control Software. All spectra were collected with a laser excitation of 532 nm, a black-illuminated CCD camera, and a 60× water immersion objective (Nikon Fluor; NA = 1). All spectra were collected in the range 3670 – 0 cm^{-1}, with a spectral resolution of 3 cm^{-1}. The spatial resolution possible to achieve with this setup is approximately 0.36 μm. The size of the mapped area was dependent on cell size and was adjusted individually. The sampling density for measured cells was 0.5 – 0.6 μm depending on cell size and the integration time, i.e. 0.5 s and 0.1 s for fixed and live cells, respectively. Analysis of Raman imaging data enables the creation of Raman images based on the integral intensity of selected bands, showing the distribution of cellular components, i.e. organic matter (3015 – 2815 cm^{-1}), lipids (2860 – 2840 cm^{-1}), nucleic acids (810 – 790 cm^{-1}), cytochrome *c* (750 cm^{-1}) and MitoBADY Rp (2220 cm^{-1}). From each sample, 4 – 6 cells were imaged.

2.3. Measurement of the MMP

The MMP measurements were performed using a microplate reader (BioTek). HAEC cells were cultured on 96-well cell culture plates. To measure MMP JC-1 (5,5′6,6′-tetrachloro-1,1′,3,3′- tetraethylbenzimidazolylcarbocyanine iodide, Invitrogen^{TM}) fluorescence probe was used. The cells were treated with MitoBADY (100 – 400 nM), FCCP (0.1 – 5.0 μM), rotenone (1 μM) together with antimycin A (1 μM), oligomycin (1 μM), and stress hormones i.e., adrenaline (5 μM), noradrenaline (5 μM), cortisol (5 nM) and their equimolar mixture (depicted as an EM). After 30 min of incubation with the tested compounds, the plates were washed with warm PBS (with the addition of Ca^{2+} and Mg^{2+} ions) and JC-1 was added for 30 min. After that, the cells were washed and imagined in a preheated HBSS (Merck).

2.4. Data analysis

Raman data were analyzed using WITec Plus software (WITec GmbH). Preprocessing of Raman spectra included Cosmic Ray Removal (CRR; filter size: 4; dynamic factor: 4) and Background Subtraction (BG; polynomial order: 3). The spectra prepared this way were analyzed by k-Means Cluster Analysis (KMCA) in the range of 1800 – 500 cm^{-1}. As a result of cluster analysis, average spectra were obtained for various cell components (i.e. cytoplasm, cell nucleus, lipids, and additionally cytoplasm region with a high content of cytochrome *c* in the case of live cells). Average Raman spectra were obtained by averaging spectra from individual classes from KMCA analysis (i.e., cytoplasm, nucleic acids, lipids, and cytochrome *c*) for 5–6 cells. The Raman spectra presented here are shown in the range of 3050 – 500 cm^{-1} and were normalized using the Opus software (Bruker). For data presentation Origin 2021 (OriginLab Corporation) and GraphPad Prism 9 (GraphPad Software) were used.

3. Results and discussion

3.1. Visualization of mitochondria in endothelial cells

Detection of mitochondria in the ECs was performed in live and fixed cells using the label-free RM approach. Raman spectra of live HAEC are characterized by the intense resonance Raman bands at 1586, 1315, 1175, 1130, and 750 cm^{-1} (Fig. 2A), which are markers of hemoproteins [35], assigned mainly to cytochrome *c* in the reduced form [36]. Low intensity of these bands in the Raman spectrum of fixed cells results from its change into the oxidized form of cytochrome *c* (Fig. 2B) [18].

During the electron transport, cytochrome *c* changes the oxidation state of the iron located in the center of the heme group, from Fe^{3+} to Fe^{2+} state, and after donating the electron to the next carrier, the iron atom returns to the Fe^{3+} state [10]. The Raman spectrum of cytochrome *c* depends on the oxidation state of the heme iron as well as the protein concentration. The reduced cytochrome *c* is often considered as a marker of mitochondrial activity [18] and its Raman signal is used for imaging the distribution of mitochondria [25]. As can be seen (Fig. 2A-B), live cells exhibit high mitochondrial activity, unlike the fixed ones.

One of the main goals of this work was to visualize the mitochondria in the ECs. For this purpose, labeled Raman imaging was applied. It was necessary to optimize MitoBADY concentrations and incubation time to avoid its non-specific accumulation in cells. The analysis was performed on live cells to ensure high mitochondrial activity. It was aimed to find the minimal concentration and incubation time sufficient to detect the probe in cells. First, the optimal concentration was defined, at which the characteristic band of MitoBADY (2220 cm^{-1}) was noticed in the Raman spectrum of ECs. KMCA gave the image and average spectra of the characterized classes (Fig. 3A-B), the most important of which was the cytoplasm class (whole-cell without the nucleus), which was further analyzed to provide information about the changes in the MitoBADY band intensity. The tested concentrations of MitoBADY ranged from 50 to 400 nM, and the lowest one detected in ECs was determined based on KMCA as 100 nM (Fig. 3C-D). After determining the optimal concentration of MitoBADY, the effect of the incubation time was monitored, after 15, 30, and 60 min. Already after 15 min of incubating cells with MitoBADY, the spectra showed a band at 2220 cm^{-1}, but its intensity was so weak that 30 min of incubation was used for further analysis. Moreover, 30 min of incubation gave the best co-localization with cytochrome *c* (Fig. 3C and 3E).

As with live cells, the same procedure was applied for fixed cells. In this case, the optimal conditions to detect MitoBADY in ECs were estimated as a concentration of 400 nM and a 60 min incubation time (Fig. S1). Notably, the concentration and incubation time for live and fixed cells differ from each other, i.e. to detect MitoBADY in fixed ECs requires a higher concentration and a longer incubation time. However, in the latter case, MitoBADY shows distribution not only of mitochondria but also of other lipidic structures, to which it has an affinity.

3.2. Raman spectral signature of the membrane potential of mitochondria

One of the most important indicators of mitochondrial dysfunction is the depolarization of the mitochondrial membrane. In this work, we tested the effect of selected compounds that are known to alter the membrane potential of mitochondria. FCCP (carbonyl cyanide 4-

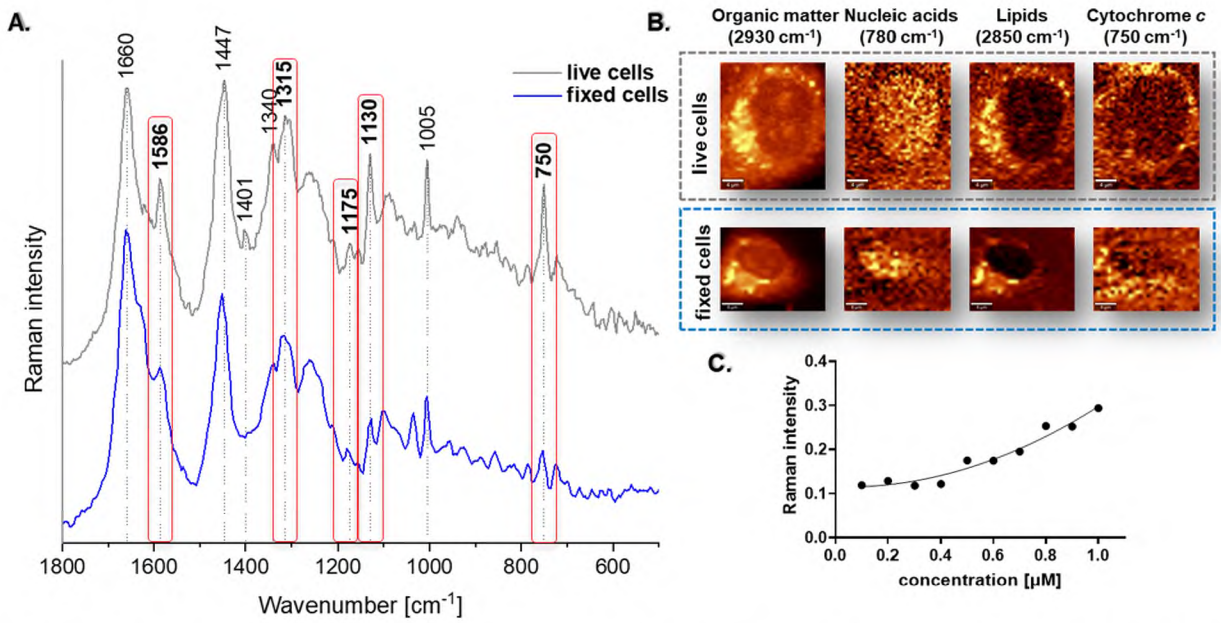

Fig. 2. **A.** The averaged spectra of cytoplasm region of live (grey) and fixed (blue) HAEC. Bands characteristic of cytochrome *c* are in the red frame. **B.** Raman images of live (grey) and fixed (blue) HAEC obtained by the integration of selected Raman bands: 2930 cm^{-1} (organic matter), 780 cm^{-1} (nucleic acids) 2950 cm^{-1} (lipids), and 750 cm^{-1} (cytochrome *c*). **C.** Standard curve for cytochrome *c* band at 750 cm^{-1}. (For interpretation of the references to colour in this figure legend, the reader is referred to the web version of this article.)

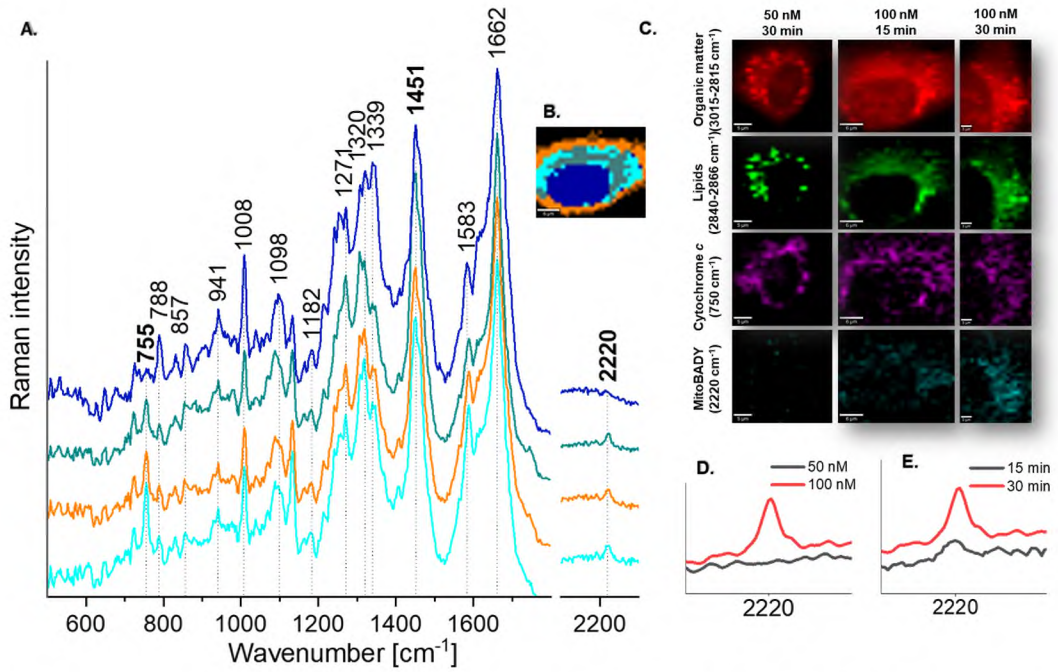

Fig. 3. **A.** KMCA-based average spectra of characteristic classes (a. nucleus, b. cytoplasm region with high content of lipids, c. organic matter, d. cytoplasm region with high content of cytochrome *c*) and **B.** cluster maps, the most important of which was the cytoplasm class. Raman imaging of live HAEC cells incubated with MitoBADY. **C.** Selected experimental conditions: 50 nM, 30 min; 100 nM, 15 min; 100 nM, 30 min, obtained by the integration of Raman bands over the selected Raman bands at: 2930 cm^{-1} (organic matter), 2850 cm^{-1} (lipids), 750 cm^{-1} (cytochrome *c*) and 2220 cm^{-1} (MitoBADY). Average spectrum showing the differences between the 2220 cm^{-1} band intensity for **D.** concentration and **E.** incubation time.

(trifluoromethoxy)phenylhydrazone) belongs to a group of compounds called uncouplers, that transfer protons from the intermembrane space to the mitochondrial matrix, which in turn reduces the MMP and reduces the proton gradient in the inner mitochondrial membrane [37]. In addition, several selected compounds were used that directly inhibit electron transport in ETC and the synthesis of ATP. Rotenone is a highly specific inhibitor of complex I, that blocks the accumulation of protons in the intermembrane space [9]. In turn, antimycin A inhibits complex III, distorting the proton gradient and hence the loss of the MMP [38]. Altogether, the use of rotenone and antimycin A inhibits electron transport in mitochondria. Oligomycin, an inhibitor of the V complex, contributes to the accumulation of protons in the mitochondrial intermembrane space, the hyperpolarization of the mitochondrial membrane, and slowing down the electron transport chain [9,37]

subsequently, disturbing the synthesis of ATP. To inhibit complex IV of the mitochondrial respiratory chain, sodium azide was used. It is a commonly used compound that binds to the hem group in cytochrome *c* (reduced electron carrier) stopping the redox reaction in the electron transport chain. As a consequence, decreased ATP production, slow-down of ETC, and accumulation of the reduced form of cytochrome *c* and ROS are observed [39].

In order to establish the influence of the above-mentioned compounds on the Raman signature of ECs, we decided to use a semi-quantitative analysis based on the ratio of the selected Raman bands. As reported [40,41], the intensity of resonance Raman bands is not linearly correlated with the concentration of the observed specimen, therefore the analysis of the relative spectral intensity must be carried out with special care (Fig. 2C). The cytochrome *c* oxidation state, together with changes in the conformational state [41] and the molecular dynamics of apoptotic cells [42], can be determined with rRS. The previously reported approach for quantification of relative cytochrome *c* content was based on the normalized resonance Raman bands, with the intensity of bands at 1004 cm^{-1} (protein) [43], 1450 cm^{-1} (protein and lipids) [43], and 1652 cm^{-1} (protein and lipids) [44]. In this work, for normalization, we selected the Raman band at 1450 cm^{-1}, which results from CH_2/CH_3 bending vibrations of lipids and proteins, and therefore its intensity comes from the majority of cell components.

For the estimation of MMP, the fluorescence intensity of JC-1 dye was analyzed. The relative MMP is expressed as the ratio of the fluorescence at 590 nm (red), when the potential is high, to the fluorescence at 527 nm (green), when the potential is low. Mitochondrial membrane depolarization is demonstrated by a decrease in the red to green fluorescence intensity ratio.

We applied FCCP to live HAEC at the concentration of 0.7 mM (average Raman spectrum shown in Fig. 4A) to observe a decrease in MMP. FCCP-induced uncoupling of the electron transport leads to a decrease in the relative amount of reduced electron carriers, including cytochrome *c*. As expected, we observed a decrease in the ratio of integral intensity cytochrome *c* bands at 750/1450 cm^{-1} under the FCCP (0.7 μM, 15 min) treatment (Fig. 4B). The acquired results correspond to those obtained for JC-1 staining (Fig. 4C).

In the next step, the action of inhibitors i.e. rotenone with antimycin A, and oligomycin was evaluated in live HAEC using the same approach. The concentration (1 μM) of inhibitors was set based on [45] and cells were incubated for 30 min. The band at 750 cm^{-1} (to the band at 1450 cm^{-1}) experienced a slight decrease in intensity due to the action of rotenone and antimycin A, and the increase after treatment with oligomycin (Fig. 4B). Cytochrome *c* was reported to be a reliable redox indicator that reflects mitochondria activity [18]. Rotenone together with antimycin A reduces mitochondrial activity caused by the slow-down or inhibition of the electron transport chain, while oligomycin, by inhibiting the synthesis of ATP, causes hyperpolarization. The Raman data were compared with those obtained for JC-1 staining (Fig. 4C). These results confirmed the action of the tested compounds, where antimycin A and rotenone caused depolarization of the mitochondrial membrane, and oligomycin showed an opposite effect leading to membrane hyperpolarization. Average spectra are shown in Fig. 5A.

Here we also analyzed the Raman spectra of EC incubated with sodium azide (NaN_3, 10 mM) (Fig. 4D) using the same approach i.e. calculating the integral intensity ratio of bands at 750/1450 cm^{-1} (Fig. 4E). As the incubation time of the cells with the azide increases, an increase in the ratio of the band at 750 cm^{-1} to the reference band is observed. The inhibition of complex IV by NaN_3 leads to the increase in the relative amount of reduced electron carrier, i.e. cytochrome *c*. Since the redox reaction is stopped, it causes the accumulation of the reduced form of cytochrome *c*. Subsequently, the longer the incubation time, the longer the redox reaction is stopped and more cytochrome *c* accumulates until the NaN_3 causes cell death and loss of signal from cytochrome *c* (approx. after 30 min).

To test whether the MitoBADY could be used as a probe to track changes in the MMP, a number of compounds with different effects on mitochondria were used.

The live cells were treated with 1 μM rotenone and antimycin A (30 min), or 1 μM oligomycin (30 min), or 0.7 μM FCCP (15 min), and their average spectra are shown in Fig. 5A. Then, the medium was changed and MitoBADY was added for the next 30 min. The results obtained for

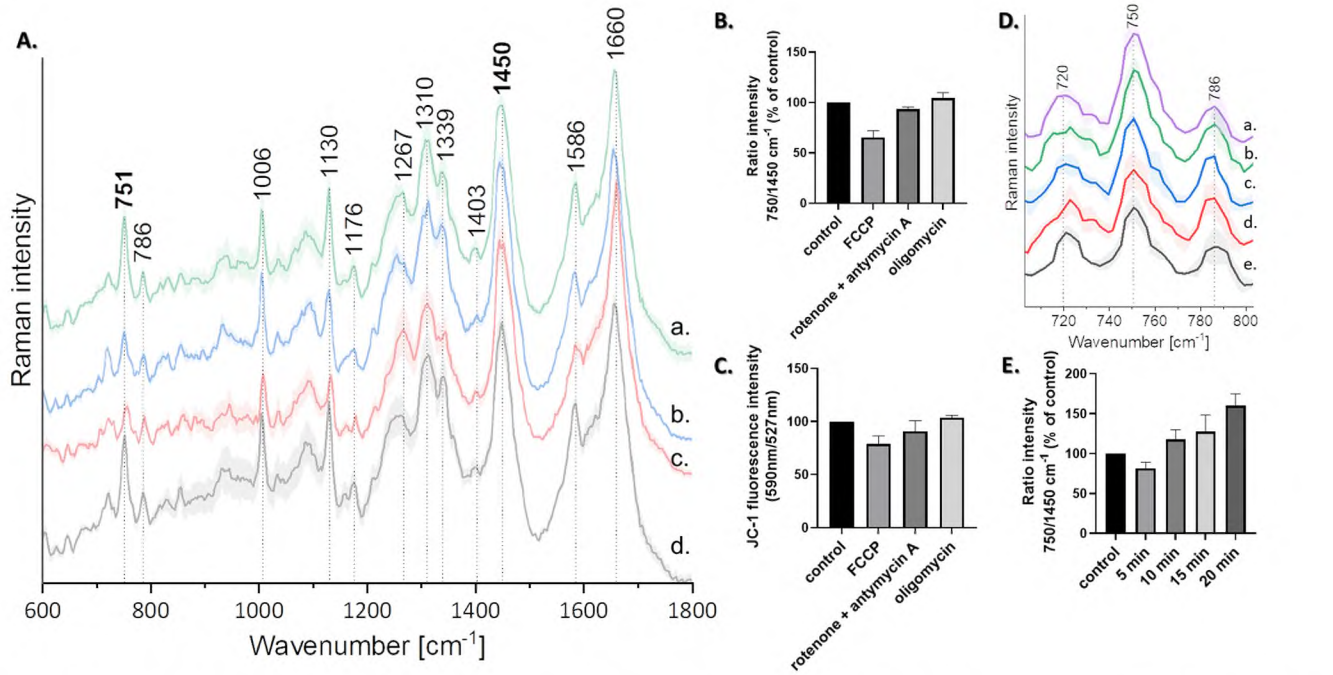

Fig. 4. A. Averaged Raman spectra of cytoplasm region with standards deviation for oligomycin (a), rotenone and antimycin A (b), FCCP (c), and control (d). **B.** The integral intensity ratio of bands at 750/1450 cm^{-1}. **C.** The JC-1 fluorescence intensity (ratio of 590 nm/527 nm). **D.** Average spectrum showing the differences between the 750 cm^{-1} band intensity after incubation with 10 mM NaN_3 (a. 20 min, b. 15 min, c. 10 min, d. 5 min, e. control). **E.** The integral intensity ratio of bands at 750/1450 cm^{-1}.

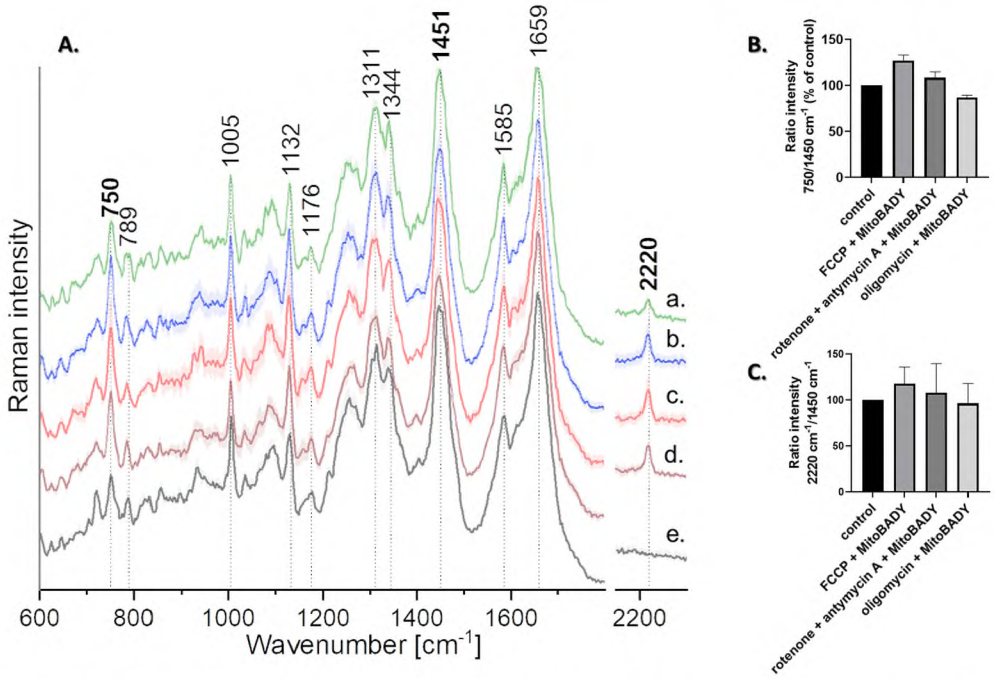

Fig. 5. A. Averaged Raman spectra of cytoplasm region with standards deviation for oligomycin + MitoBADY (a), rotenone and antimycin A + MitoBADY (b), FCCP + MitoBADY (c), MitoBADY (d) and control (e.). **B.** The integral intensity ratio of bands at 750/1450 cm^{-1}. **C.** The integral intensity ratio of bands at 2220/1450 cm^{-1}.

samples that were incubated additionally with MitoBADY differ from those where cells were incubated only with rotenone + antimycin A, or oligomycin, or FCCP. The reverse relationship in the ratio 750/1450 cm^{-1} has been shown (Fig. 4C and 5C). By calculating the ratios of the bands 2220/1450 cm^{-1} (Fig. 5C) and 750/1450 cm^{-1} (Fig. 5B), an increase in these values can be seen for samples treated with the rotenone and antimycin A, and with FCCP, and a decrease for oligomycin treated cells, which corresponds to hyperpolarization and depolarization, respectively. In its structure, MitoBADY contains a positively charged TTP^{+} group through, which is a targeting group for the mitochondrial membrane. When the mitochondrial membrane is depolarized, i.e. the accumulation of protons is stopped (by adding rotenone + antimycin A, or FCCP), we observed an increase in the Rp accumulation in the membrane, which is manifested by the higher ratio of bands at 2220/1450 cm^{-1}, in respect to control. When the membrane is hyperpolarized (by oligomycin), the accumulation of MitoBADY in the membrane is reduced. Comparing the ratio of the bands at 750/1450 cm^{-1} (Fig. 4C), we observe the opposite relation than in the case of the ratio of the bands at 2220/1450 cm^{-1} (Fig. 5C). We hypothesize that the TPP^{+} present in the molecular structure of MitoBADY may decrease the MMP. Changes in ETC caused by FCCP, rotenone, antimycin A and oligomycin, contribute to MMP, and membrane depolarization or hyperpolarization has a significant impact on the accumulation of MitoBADY in the mitochondria.

3.3. *Do stress hormones affect the mitochondrial membrane potential in EC?*

It was reported that the secretion and turnover of stress hormones are associated with mitochondria located in various tissues [12]. However, their effect on endothelial mitochondria is still not well recognized. Here, we attempt to understand the effect of stress hormones such as adrenaline, noradrenaline, cortisol, and the equimolar mixture (EM) of these three hormones on the MMP by looking at the cytochrome *c* Raman signal. To understand the relation between the MMP (an indicator of mitochondrial activity) and cytochrome *c*, we applied the same approach as described above. The use of the JC-1 dye allowed us to observe the change in MMP, while the intensity of the bands was determined based on the integrated intensity ratio of bands at 750/1450 cm^{-1}.

Adrenaline and noradrenaline affected the mitochondria, which can be seen as an increase in the intensity of the cytochrome *c* band. This increased mitochondrial activity was observed also when cells were treated with the EM. It was reported that adrenaline stimulates the production of cyclic adenosine monophosphate (cAMP), which is converted from ATP, while the other catecholamine hormone, i.e. noradrenaline, was not that potent (data from HMEC-1 cells) [46]. The need for more ATP, which is converted into cAMP is associated with a more ETC activity. Furthermore, the increased level of cAMP causes the activation of cAMP-dependent protein kinase, and stimulates the action of ETC (complexes II-IV), increasing mitochondrial activity at the same time [47]. In terms of cortisol, slight changes were seen compared to control (Fig. 6A). The ratio of bands 750/1450 cm^{-1} experienced an increase after treatment with remaining stress hormones (Fig. 6A). Those results are similar to those obtained after incubation with oligomycin, an antibiotic, that hyperpolarized MMP. The results correspond to those obtained from the staining with JC-1 dye (Fig. 6B), in the case of adrenaline, noradrenaline, and the EM, a higher ratio is observed than in the case of the control, which indicates membrane hyperpolarization, where it should be noted that with the sample incubated with all hormones, hyperpolarization is the highest, which may indicate interdependent effects of stress hormones. For the comparison, the Raman spectra of cells treated with stress hormones are presented in Fig. 6C.

In addition, to better understand the effect of stress hormones on mitochondrial activity, MitoBADY as a potential probe to detect changes in MMP was used. Cells incubated with stress hormones and MitoBADY (Fig. 7A) show an increased ratio of 750/1450 cm^{-1} for control (Fig. 7B), which may indicate hyperpolarization of the membrane, but the trend is parallel to that in the case of the hormones themselves (Fig. 6A). We assume that since incubation with hormones alone causes the membrane to hyperpolarize, adding a Rp would result in a lower accumulation of MitoBADY, like in the case of oligomycin. But stress hormones have a much more complex path of their action on mitochondria. The most prominent differences in ratios of 2220/1450 cm^{-1}

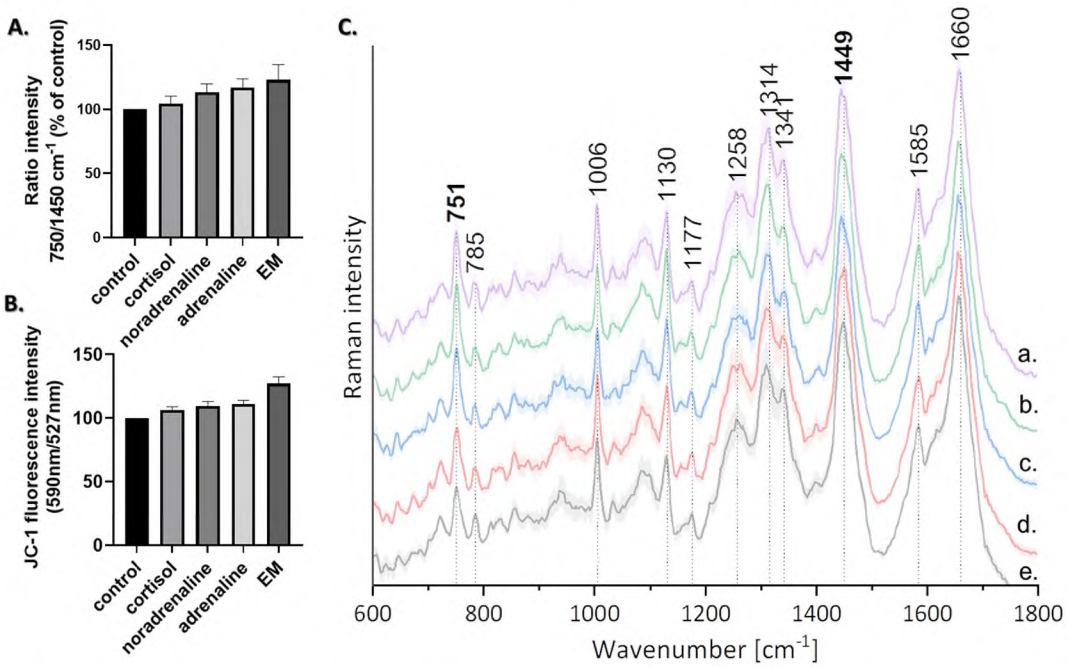

Fig. 6. A. The integral intensity ratio of bands at 750/1450 cm^{-1}. **B.** The JC-1 fluorescence intensity (ratio of 590 nm/527 nm). **C.** Averaged Raman spectra of cytoplasm region with standards deviation for EM (a), adrenaline (b), noradrenaline (c) cortisol (d), and control (e.).

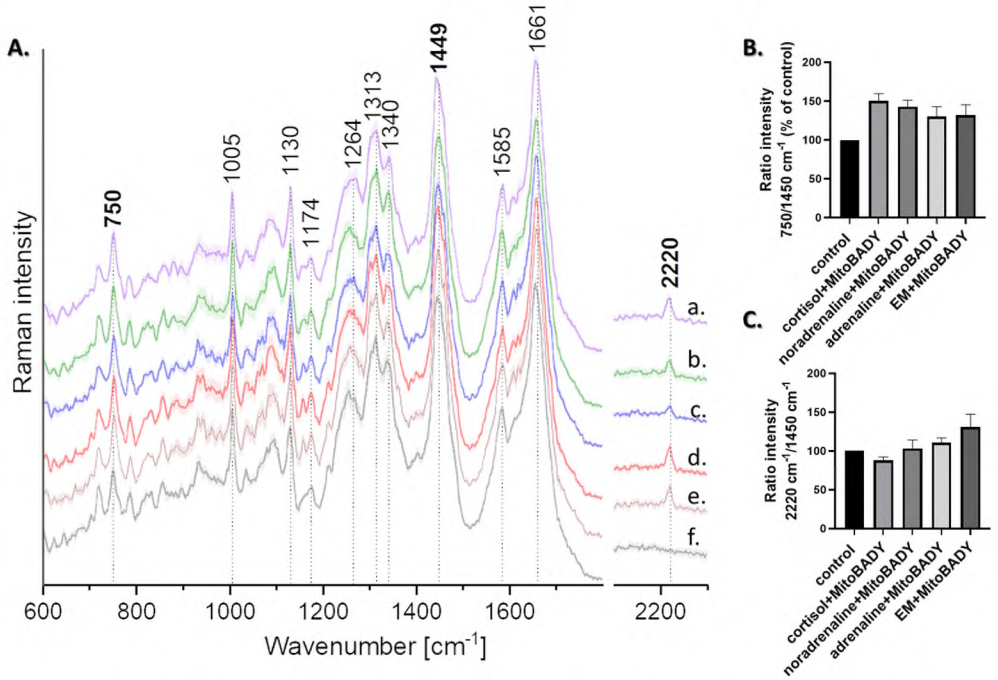

Fig. 7. A. Averaged Raman spectra of cytoplasm region with standards deviation for EM + MitoBADY (a), adrenaline + MitoBADY (b), noradrenaline + MitoBADY (c), cortisol + MitoBADY (d), MitoBADY (e.) and control (f.). **B.** The integral intensity ratio of bands at 750/1450 cm^{-1}. **C.** The integral intensity ratio of bands at 2220/1450 cm^{-1}.

and 750/1450 cm^{-1} after incubation with hormones and MitoBADY can be observed in the case of cortisol. The inverse relationship can be explained by the influence of the hormone on the electron transport chain. It was reported, that cortisol increases the efficiency of the respiratory chain by influencing complex I in the mitochondria of the rat brain [11]. Increasing the efficiency of ETC causes increased mitochondria activity, seen as an increase in the 750/1450 cm^{-1} (Fig. 7B) band ratio. On the other hand, looking at the band ratio of 2220/1450 cm^{-1} (Fig. 7C) we can see that the dependence shows a different action to the introduction of a hormone, e.g. a specific interaction with the mitochondrial membrane. It can be postulated that the influence of hormones on the potential of the mitochondrial membrane is much weaker and more intricate than in the case of the other compounds discussed in this paper (FCCP, rotenone, antimycin A and oligomycin). That could explain the different trends for hormones and others discussed here agents, of the ratios of 2220/1450 cm^{-1} and 750/1450 cm^{-1}

bands after additional incubation with MitoBADY. Further detailed research is going to be carried out.

4. Conclusions

In this work, we examined the applicability of MitoBADY (Rp) as a marker of mitochondrial activity and how to make reliable measurements of mitochondrial activity using this Rp. We also determined that MitoBADY provides information about MMP in ECs. We optimized the conditions for using MitoBADY in live and fixed ECs. Notably, the concentration and incubation time for live and fixed cells vary from each other, i.e. to measure MitoBADY in fixed EC a higher concentration and longer incubation time are required. However, in that condition, MitoBADY distribution is not specific only to mitochondria but also to lipids in general. Since the integrity of mitochondrial function is fundamental to cells, such analysis should be performed on live cells, not fixed ones. We used a quantitative approach based on the ratios of the bands at 750 cm^{-1} and 1450 cm^{-1} to estimate the relative amount of cytochrome *c* in ECs, which is a known marker of mitochondria activity. This approach was applied to live cells treated with mitochondria uncoupler and compounds affecting electron transport in ETC. We observed changes occurring in mitochondria as a slowdown of the ETC (hyperpolarization) and distortion of the proton gradient in the intermembrane space (depolarization). For that purpose, FCCP, rotenone, antimycin A (depolarization), and oligomycin (hyperpolarization) were used. Moreover, changes in the MMP were recognized also by using Rp. The last but not least, the effect of stress hormones on ECs was shown. The observed changes suggest that hormones cause an increase in MMP, in particular, when cells were treated with an equimolar mixture of them.

CRediT authorship contribution statement

Anna Pieczara: Conceptualization, Data curation, Formal analysis, Investigation, Visualization, Writing – original draft. **Ewelina Matuszyk:** Conceptualization, Data curation, Investigation, Writing – original draft. **Piotr Szczesniak** Investigation. **Jacek Mlynarski:** Supervision, Investigation. **Malgorzata Baranska:** Conceptualization, Investigation, Supervision, Writing – review & editing.

Declaration of Competing Interest

The authors declare that they have no known competing financial interests or personal relationships that could have appeared to influence the work reported in this paper.

Acknowledgments

This work was supported by a grant from the National Science Center Poland (NCN) (OPUS15 no. UMO-2018/29/B/ST4/00335 to MB).

The authors are grateful to Ph.D. Patrycja Kaczara for supplying some of the reagents and valuable help in the interpretation of the results, and MSc Renata Budzynska (JCET UJ) for cell culture maintenance.

Appendix A. Supplementary data

Supplementary data to this article can be found online at https://doi.org/10.1016/j.saa.2022.121978.

References

[1] W.C. Aird, Phenotypic heterogeneity of the endothelium: I. Structure, function, and mechanisms, Circ. Res. 100 (2007) 158–173, https://doi.org/10.1161/01.RES.0000255691.76142.4a.

[2] X. Tang, Y.X. Luo, H.Z. Chen, D.P. Liu, Mitochondria, endothelial cell function, and vascular diseases, Front. Physiol. 5 MAY (2014) 175. https://doi.org/10.3389/fphys.2014.00175.

[3] S. Wisnovsky, E.K. Lei, S.R. Jean, S.O. Kelley, Mitochondrial Chemical Biology: New Probes Elucidate the Secrets of the Powerhouse of the Cell, Cell, Chem. Biol. 23 (2016) 917–927, https://doi.org/10.1016/j.chembiol.2016.06.012.

[4] S. Javadov, A.V. Kozlov, A.K.S. Camara, Mitochondria in Health and Diseases, Cells. 9 (2020) 1177, https://doi.org/10.3390/cells9051177.

[5] A. Szewczyk, W. Jarmuszkiewicz, A. Koziel, I. Sobieraj, W. Nobik, A. Lukasiak, A. Skup, P. Bednarczyk, B. Drabarek, D. Dymkowska, A. Wrzosek, K. Zablocki, Mitochondrial mechanisms of endothelial dysfunction, Pharmacol. Rep. 67 (2015) 704–710, https://doi.org/10.1016/j.pharep.2015.04.009.

[6] M.A. Kluge, J.L. Fetterman, J.A. Vita, Mitochondria and endothelial function, Circ. Res. 112 (2013) 1171–1188, https://doi.org/10.1161/CIRCRESAHA.111.300233.

[7] X. Tang, Y.X. Luo, H.Z. Chen, D.P. Liu, Mitochondria, endothelial cell function, and vascular diseases, Front. Physiol. 5 MAY (2014). https://doi.org/10.3389/fphys.2014.00175.

[8] S. Caja, J.A. Enríquez, Mitochondria in endothelial cells: Sensors and integrators of environmental cues, Redox Biol. 12 (2017) 821–827, https://doi.org/10.1016/j.redox.2017.04.021.

[9] N.A. Brazhe, E.I. Nikelshparg, A.A. Baizhumanov, V.G. Grivennikova, A. A. Semenova, S.M. Novikov, V.S. Volkov, A.V. Arsenin, D.I. Yakubovsky, A. B. Evlyukhin, Z.V. Bochkova, E.A. Goodilin, G.V. Maksimov, O. Sosnovtseva, A. B. Rubin, SERS uncovers the link between conformation of cytochrome c heme and mitochondrial membrane potential, BioRxiv. (2021), https://doi.org/10.1101/2021.01.03.425119.

[10] V.W.. Rodwell, D. Bender, K.M.. Botham, P.J.. Kennelly, P.A. Weil, Biochemia Harpera ilustrowana, 7th ed., PZWL Wydawnictwo Lekarskie, Warszawa, 2018.

[11] M. Picard, B.S. McEwen, Psychological Stress and Mitochondria: A Systematic Review, Psychosom. Med. 80 (2018) 141–153, https://doi.org/10.1097/PSY.0000000000000545.

[12] M. Picard, B.S. McEwen, E.S. Epel, C. Sandi, An energetic view of stress: Focus on mitochondria, Front. Neuroendocrinol. 49 (2018) 72–85, https://doi.org/10.1016/j.yfrne.2018.01.001.

[13] S. Ranabir, K. Reetu, Stress and hormones, Indian J. Endocrinol. Metab. 15 (2011) 18, https://doi.org/10.4103/2230-8210.77573.

[14] L.D. Sher, H. Geddie, L. Olivier, M. Cairns, N. Truter, L. Beselaar, M.F. Essop, Chronic stress and endothelial dysfunction: Mechanisms, experimental challenges, and the way ahead, Am. J. Physiol. - Hear. Circ. Physiol. 319 (2020) H488–H506, https://doi.org/10.1152/ajpheart.00244.2020.

[15] C. Cottet-Rousselle, X. Ronot, X. Leverve, J.F. Mayol, Cytometric assessment of mitochondria using fluorescent probes, Cytom. Part A. 79 A (2011) 405–425. https://doi.org/10.1002/cyto.a.21061.

[16] P.M. Schaefer, S. Kalinina, A. Rueck, C.A.F. von Arnim, B. von Einem, NADH Autofluorescence—A Marker on its Way to Boost Bioenergetic Research, Cytom. Part A 95 (2019) 34–46, https://doi.org/10.1002/cyto.a.23597.

[17] K. Alm, Z. El-Schich, M. Falck, A. Gjrloff Wingren, B. Janicke, S. Oredsso, Cells and Holograms – Holograms and Digital Holographic Microscopy as a Tool to Study the Morphology of Living Cells, in: Hologr. - Basic Princ. Contemp. Appl., IntechOpen, 2013. https://doi.org/10.5772/54505.

[18] T. Morimoto, L. Da Chiu, H. Kanda, H. Kawagoe, T. Ozawa, M. Nakamura, K. Nishida, K. Fujita, T. Fujikado, Using redox-sensitive mitochondrial cytochrome Raman bands for label-free detection of mitochondrial dysfunction, Analyst. 144 (2019) 2531–2540, https://doi.org/10.1039/c8an02213e.

[19] M. Kakita, M. Okuno, H.O. Hamaguchi, Quantitative analysis of the redox states of cytochromes in a living L929 (NCTC) cell by resonance Raman microspectroscopy, J. Biophotonics. 6 (2013) 256–259, https://doi.org/10.1002/jbio.201200042.

[20] Z. Zhao, Y. Shen, F. Hu, W. Min, Applications of vibrational tags in biological imaging by Raman microscopy, Analyst. 142 (2017) 4018–4029, https://doi.org/10.1039/c7an01001j.

[21] H. Yamakoshi, K. Dodo, A. Palonpon, J. Ando, K. Fujita, S. Kawata, M. Sodeoka, Alkyne-tag Raman imaging for visualization of mobile small molecules in live cells, J. Am. Chem. Soc. 134 (2012) 20681–20689, https://doi.org/10.1021/ja308529n.

[22] L. Wei, F. Hu, Z. Chen, Y. Shen, L. Zhang, W. Min, Live-Cell Bioorthogonal Chemical Imaging: Stimulated Raman Scattering Microscopy of Vibrational Probes, Acc. Chem. Res. 49 (2016) 1494–1502, https://doi.org/10.1021/acs.accounts.6b00210.

[23] L. Wei, Z. Chen, L. Shi, R. Long, A.V. Anzalone, L. Zhang, F. Hu, R. Yuste, V. W. Cornish, W. Min, Super-multiplex vibrational imaging, Nature 544 (2017) 465–470, https://doi.org/10.1038/nature22051.

[24] F. Hu, C. Zeng, R. Long, Y. Miao, L. Wei, Q. Xu, W. Min, Supermultiplexed optical imaging and barcoding with engineered polyynes, Nat. Methods. 15 (2018) 194–200, https://doi.org/10.1038/nmeth.4578.

[25] K. Hamada, K. Fujita, N.I. Smith, M. Kobayashi, Y. Inouye, S. Kawata, Raman microscopy for dynamic molecular imaging of living cells, J. Biomed. Opt. 13 (04) (2008) 1, https://doi.org/10.1117/1.2952192.

[26] A.F. Palonpon, M. Sodeoka, K. Fujita, Molecular imaging of live cells by Raman microscopy, Curr. Opin. Chem. Biol. 17 (2013) 708–715, https://doi.org/10.1016/j.cbpa.2013.05.021.

[27] R. Smith, K.L. Wright, L. Ashton, Raman spectroscopy: An evolving technique for live cell studies, Analyst. 141 (2016) 3590–3600, https://doi.org/10.1039/c6an00152a.

[28] Y. Li, Z. Wang, X. Mu, A. Ma, S. Guo, Raman tags: Novel optical probes for intracellular sensing and imaging, Biotechnol. Adv. 35 (2017) 168–177, https://doi.org/10.1016/j.biotechadv.2016.12.004.

[29] E. Matuszyk, A. Adamczyk, B. Radwan, A. Pieczara, P. Szcześniak, J. Mlynarski, K. Kamińska, M. Baranska, Multiplex Raman imaging of organelles in endothelial cells, Spectrochim. Acta - Part A Mol. Biomol. Spectrosc. 255 (2021) 119658, https://doi.org/10.1016/j.saa.2021.119658.

[30] H. Yamakoshi, K. Dodo, M. Okada, J. Ando, A. Palonpon, K. Fujita, S. Kawata, M. Sodeoka, Imaging of EdU, an alkyne-tagged cell proliferation probe, by Raman microscopy, J. Am. Chem. Soc. 133 (2011) 6102–6105, https://doi.org/10.1021/ja108404p.
[31] L. Wei, F. Hu, Y. Shen, Z. Chen, Y. Yu, C.C. Lin, M.C. Wang, W. Min, Live-cell imaging of alkyne-tagged small biomolecules by stimulated Raman scattering, Nat. Methods. 11 (2014) 410–412, https://doi.org/10.1038/nmeth.2878.
[32] S. Hong, T. Chen, Y. Zhu, A. Li, Y. Huang, X. Chen, Live-Cell Stimulated Raman Scattering Imaging of Alkyne-Tagged Biomolecules, Angew, Chemie. 126 (2014) 5937–5941, https://doi.org/10.1002/ange.201400328.
[33] H. Yamakoshi, A. Palonpon, K. Dodo, J. Ando, S. Kawata, K. Fujita, M. Sodeoka, A sensitive and specific Raman probe based on bisarylbutadiyne for live cell imaging of mitochondria, Bioorg. Med. Chem. Lett. 25 (2015) 664–667, https://doi.org/10.1016/j.bmcl.2014.11.080.
[34] N. Kamo, M. Muratsugu, R. Hongoh, Y. Kobatake, Membrane potential of mitochondria measured with an electrode sensitive to tetraphenyl phosphonium and relationship between proton electrochemical potential and phosphorylation potential in steady state, J. Membr. Biol. 49 (1979) 105–121, https://doi.org/10.1007/BF01868720.
[35] E. Bik, A. Dorosz, L. Mateuszuk, M. Baranska, K. Majzner, Fixed versus live endothelial cells: The effect of glutaraldehyde fixation manifested by characteristic bands on the Raman spectra of cells, Spectrochim. Acta - Part A Mol. Biomol. Spectrosc. 240 (2020), 118460, https://doi.org/10.1016/j.saa.2020.118460.
[36] T.C. Strekas, T.G. Spiro, Cytochrome c: Resonance Raman spectra, BBA - Protein Struct. 278 (1972) 188–192, https://doi.org/10.1016/0005-2795(72)90121-3.
[37] M.R. Duchen, Mitochondria in health and disease: Perspectives on a new mitochondrial biology, Mol. Aspects Med. 25 (2004) 365–451, https://doi.org/10.1016/j.mam.2004.03.001.
[38] X. Ma, M. Jin, Y. Cai, H. Xia, K. Long, J. Liu, Q. Yu, J. Yuan, Mitochondrial electron transport chain complex III is required for antimycin A to inhibit autophagy, Chem. Biol. 18 (2011) 1474–1481, https://doi.org/10.1016/j.chembiol.2011.08.009.
[39] Y. Zuo, J. Hu, X. Xu, X. Gao, Y. Wang, S. Zhu, Sodium azide induces mitochondria-mediated apoptosis in PC12 cells through Pgc-1α-associated signaling pathway, Mol. Med. Rep. 19 (2019) 2211–2219, https://doi.org/10.3892/mmr.2019.9853.
[40] N.A. Brazhe, M. Treiman, A.R. Brazhe, N.L. Find, G. V. Maksimov, O. V. Sosnovtseva, Mapping of Redox State of Mitochondrial Cytochromes in Live Cardiomyocytes Using Raman Microspectroscopy, PLoS One 7 (2012) 41990. https://doi.org/10.1371/journal.pone.0041990.
[41] S. Berezhna, H. Wohlrab, P.M. Champion, Resonance Raman investigations of cytochrome c conformational change upon interaction with the membranes of intact and CA2+-exposed mitochondria, Biochemistry 42 (2003) 6149–6158, https://doi.org/10.1021/bi027387y.
[42] M. Okada, N.I. Smith, A.F. Palonpon, H. Endo, S. Kawata, M. Sodeoka, K. Fujita, Label-free Raman observation of cytochrome c dynamics during apoptosis, Proc. Natl. Acad. Sci. U. S. A. 109 (2012) 28–32, https://doi.org/10.1073/pnas.1107524108.
[43] N.A. Brazhe, E.I. Nikelshparg, C. Prats, F. Dela, O. Sosnovtseva, Raman probing of lipids, proteins, and mitochondria in skeletal myocytes: a case study on obesity, J. Raman Spectrosc. 48 (2017) 1158–1165, https://doi.org/10.1002/jrs.5182.
[44] A. Walter, S. Erdmann, T. Bocklitz, E.M. Jung, N. Vogler, D. Akimov, B. Dietzek, P. Rösch, E. Kothe, J. Popp, Analysis of the cytochrome distribution via linear and nonlinear Raman spectroscopy, Analyst. 135 (2010) 908–917, https://doi.org/10.1039/b921101b.
[45] A. Łukasiak, A. Skup, S. Chlopicki, M. Łomnicka, P. Kaczara, B. Proniewski, A. Szewczyk, A. Wrzosek, SERCA, complex I of the respiratory chain and ATP-synthase inhibition are involved in pleiotropic effects of NS1619 on endothelial cells, Eur. J. Pharmacol. 786 (2016) 137–147, https://doi.org/10.1016/j.ejphar.2016.05.039.
[46] A. Wiktorowska-Owczarek, M. Namiecińska, M. Berezińska, J.Z. Nowak, Characteristics of adrenaline-driven receptor-mediated signals in human microvessel-derived endothelial cells, Pharmacol. Rep. 60 (2008) 950–956.
[47] C. Szabo, Hydrogen sulfide, an endogenous stimulator of mitochondrial function in cancer cells, Cells. 10 (2021) 1–19, https://doi.org/10.3390/cells10020220.